Mathematical Biosciences 308 (2019) 1–7

Contents lists available at ScienceDirect

Mathematical Biosciences

journal homepage: www.elsevier.com/locate/mbs

# Strain state dependent anisotropic viscoelasticity of tendon-to-bone insertion

Sergey Kuznetsov, Mark Pankow, Kara Peters, Hsiao-Ying Shadow Huang*

*Mechanical and Aerospace Engineering Department, North Carolina State University, R3158 Engineering Building 3, Campus Box 7910, 911 Oval Drive, Raleigh, NC 27695, United States*

ARTICLE INFO

*Keywords:*
Functionally graded materials
Viscoelasticity
Biaxial mechanical testing
Strain-rate
Dissimilar materials interfaces

ABSTRACT

Tendon-to-bone insertion tissues may be considered as functionally-graded connective tissues, providing a gradual transition from soft tendon to hard bone tissue, and functioning to alleviate stress concentrations at the junction of these tissues. The tendon-to-bone insertion tissues demonstrate pronounced viscoelastic behavior, like many other biological tissues, and are designed by the nature to alleviate stress at physiological load rates and strains states. In this paper we present experimental data showing that under biaxial tension tendon-to-bone insertion demonstrates rate-dependent behavior and that stress-strain curves for the in-plane components of stress and strain become less steep when strain rate is increased, contrary to a typical viscoelastic behavior, where the opposite trend is observed. Such behavior may indicate the existence of a protective viscoelastic mechanism reducing stress and strain during a sudden increase in mechanical loading, known to exist in some biological tissues. The main purpose of the paper is to show that such viscoelastic stress reduction indeed possible and is thermodynamically consistent. We, therefore, propose an anisotropic viscoelasticity model for finite strain. We identify the range of parameters for this model which yield negative viscoelastic contribution into in-plane stress under biaxial state of strain and simultaneously satisfy requirements of thermodynamics. We also find optimal parameters maximizing the observed protective viscoelastic effect for this particular state of strain. This model will be useful for testing and describing viscoelastic materials and for developing interfaces for dissimilar materials, considering rate effect and multiaxial loadings.

## 1. Introduction

In this paper we consider the viscoelastic behavior of tendon-to-bone insertion (enthesis), which is a transitional tissue connecting the tendon and bone. Tendon is soft and highly anisotropic tissue, while bone is hard and isotropic [1–3], therefore, their interface is extremely prone to stress concentrations during physiological loadings like running and jumping, and even more during abrupt loadings such as impact. It is the function of the insertion site to balance the mismatch in the elastic moduli, dissipating stress away from the junction to prevent injury of the joint tissues [4,5]. This protective function is possible due to the smooth gradual transition of material properties and structural features from tendon to bone tissues, including collagen fiber orientation, mineralization level and others [1,2,6,7]. Grading of composition and material properties and its effect on the stress distribution was considered in linear [2,8] and recently in nonlinear [3] settings. Essentially, this protective mechanism should work at different complex multiaxial loading states occurring physiologically and at different loading rates. In addition, thermal stability and bending behaviors of functional graded materials were also investigated [9–16], and these developed models and analyses are helpful in better understanding of complex structural materials, such as bone tissue.

It is well known that skeletal biological tissues demonstrate a significant amount of viscoelasticity in their behavior [17–19]. In particular, the tendon to bone insertion viscoelasticity was reported in Thomopoulos et al. [5]. Moreover, this viscoelastic behavior is nonlinear, i.e. the relaxation function is strain dependent [19–25] and often anisotropic [26–29].

Typically, connective tissues are tested in a uniaxial tension setting and an increase of stress with strain-rate is observed [5,22,23,30], as schematically shown in Fig. 1. However, in our set of experiments it was consistently observed that under multiaxial load conditions (e.g., equibiaxial constant strain rate stretching), the viscoelastic response is qualitatively different, i.e., the stress-strain curve becomes less steep with increase of strain rate, which suggests that the insertion site has strain state dependent anisotropic viscoelastic behavior. We

* Corresponding author.
*E-mail address:* hshuang@ncsu.edu (H.-Y.S. Huang).

https://doi.org/10.1016/j.mbs.2018.12.007
Received 30 April 2018; Received in revised form 4 December 2018; Accepted 5 December 2018
Available online 08 December 2018
0025-5564/ 

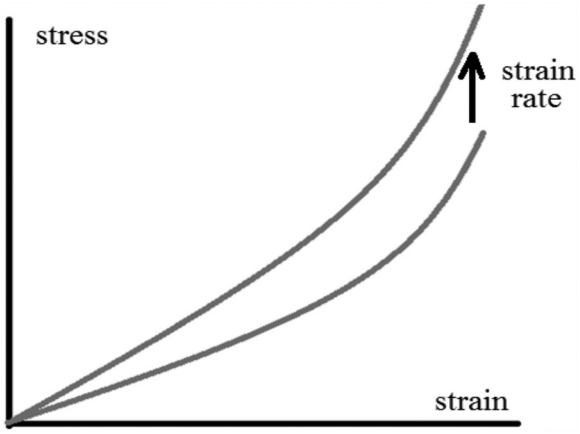


**Fig. 1.** Typical rate-dependent behavior under uniaxial tension, observed in tendons: stress level at the same strain increases with higher strain-rates.

hypothesize here that the insertion site was evolutionary designed in a way to dissipate stress more effectively under particular multiaxial "physiological" loading states at high strain-rates, and that it may not be that effective at other multiaxial strain states. To support this hypothesis we propose a thermodynamically consistent linear anisotropic viscoelasticity framework and show that observed behavior doesn't contradict requirements of thermodynamics. We note that viscoelasticity model is linear in the sense that a relaxation function doesn't depend on the strain level, at same time elastic response maybe nonlinear and capable of large deformations.

We describe next the details of experimental setup and results. A set of porcine digital flexor insertion regions was dissected from the joint, details on specimen preparation, microstructural data are presented and gripping protocols are presented in references [7] and [31]. Each specimen was subjected to equibiaxial displacement-control mechanical testing at two different strain-rates: 7%/s and 15%/s (Fig. 2). The tissue was placed so that the preferred direction of collagen fibers (transverse direction) points in the direction of *X*-axis (Fig. 2(a)). The reaction force data and displacements were recorded and the corresponding First Piola–Kirchhoff stress-true strain relationships for normal stress

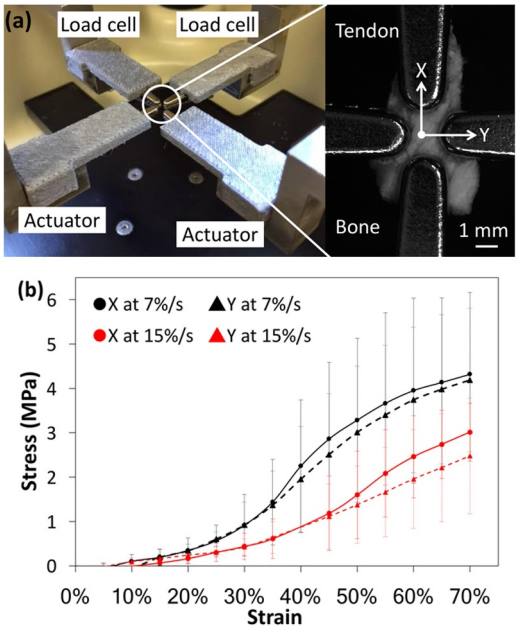


**Fig. 2.** (a) Biaxial mechanical testing setup. (b) Averaged rate-dependent response of enthesis under displacement-controlled equibiaxial extension testing at two different strain-rates.

component in *X* and *Y* directions were calculated based on the sample dimensions, the averaged over a set of 7 experiments stress-strain curves are presented on Fig. 2(b). Since tendon-to-bone insertion tissue is anisotropic, the obtained stresses in two directions were different and depicted by circles and triangles correspondingly. Black lines correspond to 7%/s strain rate, and red lines correspond to 15%/s strain-rate.

The observed stress-strain relationships were highly nonlinear. The large strains are induced mostly on the tendon, not mineralized part, while bone part experienced much lower strains [3]. The exponential growth of stresses within the 30–50% strain region may be explained by gradual recruitment of collagen fibers into tension [17,32]. The following reduction in the stress growth was probably due to the imperfect clamping and slip of the tissue (Fig. 2(b)) or due to the plasticity of damage, we are not attempting to model this behavior in this study, but concentrate our attention only on the viscoelastic response. The results also revealed a qualitatively different trend in the stress-strain relationship as the strain rate increased comparing to a typical uniaxial tension test. Namely, the results from the biaxial testing demonstrated that the increase in strain-rate caused lower stresses at the same strain level, which is opposite to what happens in a typical uniaxial tension test and points on the activation of a protective viscoelastic mechanism under equibiaxial tension conditions. The viscoelastic contribution in stress became negative, reducing the overall stress and possibly protecting the tissue from damage and rupture. Similar mechanisms are known to exist in blood vessels, where viscoelasticity reduces stress and strains of the vessel wall during a sudden mechanical loading, for example, during acute hypertension [33]. Zhang et al. [34] reported numerical simulations with a quasi-linear viscoelastic model and the viscoelasticity of arteries reduced stresses and strains, therefore increasing fatigue life of the blood vessels. To the best of our knowledge, such behavior was not observed previously in skeletal biological tissues, particularly, in tendon-to-bone insertion.

We would like to note here also that degradation of biological tissues is also known to be strain state sensitive [35–37]. Under particular ratios of principal stretches, for example, the rate of degradation of the heart valve leaflets is significantly reduced [38].

Various microscopic mechanisms may contribute to the gross behavior of the insertion tissue, including individual viscoelastic properties of collagen fibrils [39], substantial fluid flow through the fiber network due to fibers unfolding and readjustments, transient network connections – so called crosslinks, which may break and rebond during deformation and after load is removed [17,18], as shown in Fig. 3. The exact microscopic mechanism is unknown and one may only speculate that stretching tissue in the off-axial direction moves fibers (which are being stretched at same time in the axial direction) away from each

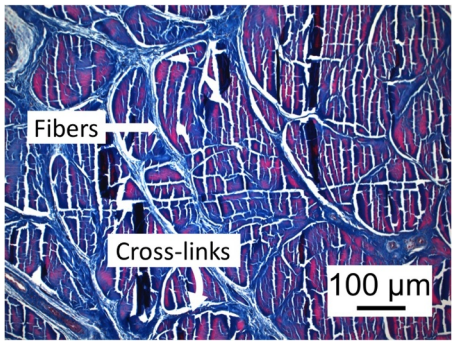


**Fig. 3.** Brightfield images at 100 x magnification (water immersion) obtained using a Zeiss Axioimager (Zeiss Inc., Germany) microscope for tendon sections. Possible microscopic mechanisms for viscoelastic behavior of soft biological tissues: viscoelasticity of components such as fibers itself and transient connections between them as well as fluid flow (white space) within fibers network.

other and breaks the cross-link bonds between them, which may restore in the new configuration, and reduces friction between unfolding collagen fibers.

Because there is no good understanding of all the underlying viscoelasticity mechanisms and how their interplay at different scales contribute to the gross viscoelasticity of biological tissues, in this paper we considered a gross phenomenological finite strain anisotropic viscoelasticity model of tendon-to-bone insertion tissue and showed that experimentally observed viscoelastic behavior may be obtained within this framework. We chose the simplest hereditary model based on the Boltzman superposition principle, also known as finite strain linear viscoelasticity [19,20,29,40], and formulated it in the reference configuration, assuming finite strains. To find parameters providing the increase of stress level, described above when increasing strain-rate under uniaxial tension (Fig. 1) and simultaneously decrease the stress level when increasing strain-rate under biaxial tension (Fig. 2(b)), we considered first uniaxial and biaxial states of strain and identified their essential differences, then we formulated a viscoelastic model and obtained parameters providing desired mechanical behaviors. Because we chose a simple superposition model, the viscoelasticity would be linear in the sense that the relaxation function did not depend on the strains magnitude. In principle, a very popular quasi-linear viscoelastic model might also be considered with the Gasser-Ogden-Holzapfel (GOH) [32] or Fung's hyperelastic function [41] for biological tissues. However, such analysis would be more complicated and less insight would be obtained, and it would still be linear that the relaxation function did not depend on the strain magnitude [22,29].

The model proposed here will be useful to analyze and characterize various viscoelastic tissues with anisotropic viscoelasticity, design materials with desired anisotropic viscoelastic behavior and to design interfaces to connect dissimilar materials, considering rate effects and multiaxial loadings.

## 2. Method

The experiments described above were conducted under different states of strain and resulted in a principally different mechanical response. In this section, we considered both states of uniaxial and biaxial strains and identified the essential differences between them. We assumed that the tendon-to-bone insertion tissue was incompressible, which is a common assumption for biological soft tissues [18]. Then for both states of strains, the deformation gradient and corresponding Green–Lagrange strain were written in a very simple form, using only one parameter – stretch λ. We assumed that stretch was a linear function of time $\lambda = \lambda(t)$ (or, equivalently, the time derivative of stretch was constant $\dot{\lambda} = const$ such that $\lambda(0) = 1$.

Consider first a homogeneous uniaxial tension in the $X$-direction of the incompressible specimen. The deformation gradient is as follows:

$$\mathbf{F}_u = \begin{bmatrix} \lambda & 0 & 0 \\ 0 & 1/\sqrt{\lambda} & 0 \\ 0 & 0 & 1/\sqrt{\lambda} \end{bmatrix} \tag{1}$$

and the corresponding Green–Lagrange strain tensor is

$$\mathbf{E}^u = \begin{bmatrix} \lambda^2 - 1 & 0 & 0 \\ 0 & 1/\lambda - 1 & 0 \\ 0 & 0 & 1/\lambda - 1 \end{bmatrix} \tag{2}$$

The first diagonal component of the strain tensor $E^u_{11} = \lambda^2 - 1$ is monotonically increasing in tension, and other two diagonal components $E^u_{22} = E^u_{33} = 1/\lambda - 1$ are monotonically decreasing.

Consider next an equibiaxial tension of an incompressible specimen in $X$ and $Y$ directions, then deformation gradient s

$$\mathbf{F}_b = \begin{bmatrix} \lambda & 0 & 0 \\ 0 & \lambda & 0 \\ 0 & 0 & 1/\lambda^2 \end{bmatrix} \tag{3}$$

and corresponding Green–Lagrange strain tensor is

$$\mathbf{E}^b = \begin{bmatrix} \lambda^2 - 1 & 0 & 0 \\ 0 & \lambda^2 - 1 & 0 \\ 0 & 0 & 1/\lambda^4 - 1 \end{bmatrix} \tag{4}$$

Here the first two diagonal components $E^b_{11} = E^b_{22} = \lambda^2 - 1$ are increasing monotonically, while the third component is decreasing monotonically. Therefore, the situation is qualitatively similar to the linear case considered [3]: if we restrict attention on the XY plane only and disregard Z-components of strain (out-of-plane), then the only difference between uniaxial and biaxial tension states is the difference in the second diagonal components: $E^b_{22}$ is an increasing function of stretch, while $E^u_{22}$ is a decreasing function of stretch; however now the components change nonlinearly with time, but still monotonic.

In the uniaxial tension (along the preferred collagen fiber direction), the other two directions are being shrunken due to the incompressibility. Neighboring collagen fibers are pushed to each other. This might increase friction between neighboring fibers while they slide and unfolded, also more cross-links may be formed. On the other hand, collagen fibers with the preferred orientation in $X$-direction are pulled away from each other in the $Y$ direction under the biaxial tension, which reduces friction and may also brake transient bonds between neighboring collagen fibers.

Next, we exploit these differences of strain states to obtain experimentally observed viscoelastic response of tendon-to-bone insertion specimen.

### 2.1. Finite strain linear viscoelasticity: Boltzmann superposition

In this section, we propose a simple anisotropic viscoelastic model based on the hereditary integral and Bolzmann Superposition principle [19,40]. We assumed additive decomposition of the second Piola–Kirchhoff stress into purely elastic and viscoelastic contributions [20,27,29,42]

$$S_{IJ} = S^e_{IJ} + S^v_{IJ}, \tag{5}$$

where the elastic contribution follows from the elastic strain energy potential,

$$S^e_{IJ} = 2\frac{\partial W(C_{IJ})}{\partial C_{IJ}} \tag{6}$$

For example, the GOH [32] model may be chosen as it was successfully used to model the anisotropic viscoelasticity of tendon-to-bone insertion with spatially graded material and structural properties [3], and the viscoelastic contribution is defined according to the Bolzmann superposition principle [40]:

$$S^v_{IJ} = \int_0^t g_{IJLK}(t-\xi)\frac{\partial E_{LK}}{\partial \xi}d\xi, \tag{7}$$

where $g_{IJLK}(t-\xi)$ is an anisotropic relaxation function.

For the uniaxial and biaxial experimental set up, the Green–Lagrange strain tensor depends on the stretch only and the time derivative may be written as

$$S^v_{IJ} = \int_0^t G_{IJLK}(t-\xi)\frac{\partial E_{LK}}{\partial \lambda}\frac{\partial \lambda}{\partial \xi}d\xi = \dot{\lambda}\frac{\partial E_{LK}}{\partial \lambda}\int_0^t G_{IJLK}(t-\xi)d\xi$$
$$= g_{IJLK}\dot{\lambda}\frac{\partial E_{LK}}{\partial \lambda}, \tag{8}$$

where the condition of a constant stretch rate $\dot{\lambda} = const$ was assumed and $g_{IJLK} = \int_0^t G_{IJLK}(t-\xi)d\xi$.

Differentiating Eqs. (2) and (4) for biaxial and uniaxial stretch tests we have following expressions:

$$\frac{\partial \mathbf{E}^b}{\partial \lambda} = 2\begin{bmatrix} \lambda & 0 & 0 \\ 0 & \lambda & 0 \\ 0 & 0 & -2/\lambda^5 \end{bmatrix} \tag{9}$$

and

$$\frac{\partial \mathbf{E}^u}{\partial \lambda} = \begin{bmatrix} 2\lambda & 0 & 0 \\ 0 & -1/\lambda^2 & 0 \\ 0 & 0 & -1/\lambda^2 \end{bmatrix}. \tag{10}$$

At this point it is convenient to rewrite stress and strain tensors in the vector notation:

$$\mathbf{S} = [S_{11}, S_{22}, S_{33}, S_{23}, S_{13}, S_{12}], \quad \mathbf{E} = [E_{11}, E_{22}, E_{33}, E_{23}, E_{13}, E_{12}]. \tag{11}$$

with

$$\frac{\partial \mathbf{E}^b}{\partial \lambda} = 2[\lambda, \lambda, -2/\lambda^5, 0, 0, 0] \tag{12}$$

and

$$\frac{\partial \mathbf{E}^u}{\partial \lambda} = 2[\lambda, -1/2\lambda^2, -1/2\lambda^2, 0, 0, 0]. \tag{13}$$

Then the stress-strain relationship may be written in the compressed matrix form as follows:

$$\mathbf{S}^v = \mathbf{g}^{'v}\frac{\partial \mathbf{E}}{\partial \lambda}\dot{\lambda}, \tag{14}$$

where $\mathbf{g}'^v$ is the constitutive 'viscoelastic matrix' matrix defining the rate-dependent component of the stress. We assume a general case of orthotropic symmetry for the viscoelastic matrix:

$$\mathbf{g}^v = \begin{bmatrix} g_{11}^{'v} & g_{12}^{'v} & g_{13}^{'v} & 0 & 0 & 0 \\ g_{11}^{v} & g_{22}^{v} & g_{23}^{v} & 0 & 0 & 0 \\ g_{13}^{'v} & g_{23}^{'v} & g_{33}^{'v} & 0 & 0 & 0 \\ 0 & 0 & 0 & g_{44}^{'v} & 0 & 0 \\ 0 & 0 & 0 & 0 & g_{55}^{'v} & 0 \\ 0 & 0 & 0 & 0 & 0 & g_{66}^{'v} \end{bmatrix} \tag{15}$$

Without loss of generality we may rewrite it as follows:

$$\mathbf{g}^{'v} = g_{11}^{'v}\mathbf{g}^v = g_{11}^{'v}\begin{bmatrix} 1 & g_{12}^{v} & g_{13}^{v} & 0 & 0 & 0 \\ g_{11}^{v} & g_{22}^{v} & g_{23}^{v} & 0 & 0 & 0 \\ g_{13}^{v} & g_{23}^{v} & g_{33}^{v} & 0 & 0 & 0 \\ 0 & 0 & 0 & g_{44}^{v} & 0 & 0 \\ 0 & 0 & 0 & 0 & g_{55}^{v} & 0 \\ 0 & 0 & 0 & 0 & 0 & g_{66}^{v} \end{bmatrix} \tag{16}$$

The matrix $\mathbf{g}^v$ should be positive semi-definite to satisfy the requirements of thermodynamics [43,44], i.e., all eigenvalues from Eq. (16) should be positive.

We note immediately that if $\mathbf{g}^{'v} = g_{11}^{'v}\mathbf{I}$, where $\mathbf{I}$ is a $6 \times 6$ unity matrix, then on one hand $g_{11}^{'v}$ should be positive to satisfy thermodynamic requirement, on the other hand, only negative $g_{11}^{'v}$ would result in negative viscoelastic contributions in stress values under biaxial tension (the stress contribution would be negative in uniaxial stress as well), which contradicts the first condition. It suggests that it is not possible to obtain the desired effects in the realm of isotropic viscoelasticity. Therefore, we considered anisotropic cases in the next section.

### 2.2. Tailoring the anisotropic viscoelastic matrix

In this section, we investigate if it is possible to identify coefficients of the matrix $\mathbf{g}^v$that yield positive, rate-dependent contribution of stresses under uniaxial tension and a negative contribution of stresses under biaxial testing for all values of λ within limits $1 \le \lambda \le \lambda_{max}$. With the lower limit, we restrict our attention only on the tension test; with the upper limit we include physiological loading of the tendon-to-bone insertion tissues [22]. To do so, we first explicitly wrote rate-dependent stresses for both tests. For the uniaxial tension,

$$\mathbf{S}^{uv} = 2\lambda\begin{bmatrix} 1 - g_{12}/2\lambda^3 - g_{13}/2\lambda^3 \\ g_{12} - g_{22}/2\lambda^3 - g_{23}/2\lambda^3 \\ g_{13} - g_{23}/2\lambda^3 - g_{33}/2\lambda^3 \\ 0 \\ 0 \\ 0 \end{bmatrix} \tag{17}$$

and for biaxial tension,

$$\mathbf{S}^{bv} = 2\lambda\begin{bmatrix} 1 + g_{12} - 2g_{13}/\lambda^6 \\ g_{12} + g_{22} - 2g_{23}/\lambda^6 \\ g_{13} + g_{23} - 2g_{33}/\lambda^6 \\ 0 \\ 0 \\ 0 \end{bmatrix} \tag{18}$$

The described uniaxial behavior implies the positive viscoelastic contribution into stress components (condition 1) is as follows:

$$c_1 = S_1^{uv}/2\lambda = 1 - g_{12}/2\lambda^3 - g_{13}/2\lambda^3 > 0 \tag{19}$$

The other stress components are typically unknown in the uniaxial test and not relevant for our purposes. Biaxial behavior implies that negative viscoelastic stress components $S_1^{bv}$ and $S_2^{bv}$(condition 2 and condition 3) could be written as follows:

$$c_2 = S_1^{bv}/2\lambda = 1 + g_{12} - 2g_{13}/\lambda^6 < 0 \tag{20}$$

$$c_3 = S_2^{bv}/2\lambda = g_{12} + g_{22} - 2g_{23}/\lambda^6 < 0, \tag{21}$$

while other components are unknown and not relevant.

Therefore, to obtain experimentally observed viscoelastic behavior conditions $c_1$, $c_2$ and $c_3$, additionally to the semi-positive definiteness of the viscoelasticity matrix, $\mathbf{g}^v$ must be satisfied for all possible values of stretch $1 \le \lambda \le \lambda_{max}$. From the forms of $c_1 - c_2$ Eqs. (19) and (20), we can see that terms with coefficient $g_{12}$ change signs if the state of strain is switched from the biaxial to the uniaxial stretches with a negative sign in $c_1$ in the uniaxial tension and with positive sign in $c_2$ and $c_3$ in biaxial tensions. Therefore, to obtain the described experimental behavior, $g_{12}$ should be negative and as large as possible in its magnitude. Terms with coefficients $g_{13}$, $g_{23}$ contribute with negative sign in both biaxial and uniaxial tension, and increasing their values would also contribute to the negative viscoelastic stress under biaxial tension.

**Case 1**

First, we consider the simplest possible case with $g_{12} < 0$, $g_{13} = g_{23} = 0$. The matrix $\mathbf{g}^v$ takes form as follows:

$$\mathbf{g}^v = g_{11}^{'v}\begin{bmatrix} 1 & g_{12}^{v} & 0 & 0 & 0 & 0 \\ g_{12}^{v} & 1 & 0 & 0 & 0 & 0 \\ 0 & 0 & 1 & 0 & 0 & 0 \\ 0 & 0 & 0 & g_{44}^{v} & 0 & 0 \\ 0 & 0 & 0 & 0 & g_{55}^{v} & 0 \\ 0 & 0 & 0 & 0 & 0 & g_{66}^{v} \end{bmatrix} \tag{22}$$

Its eigenvalues are

$$\eta = [1, 1 - g_{12}, 1 + g_{12}, g_{44}, g_{55}, g_{66}] \tag{23}$$

To keep all eigenvalues positive, the condition $|g_{12}| \le 1$ must hold. However, if we look now at conditions $c_1 - c_3$ Eqs. (19)–(21):

$$c_1 = 1 - g_{12}/2 > 0 \tag{24}$$

$$c_2 = c_3 = 1 + g_{12} < 0 \tag{25}$$

They may not be satisfied simultaneously, and the desired viscoelastic behavior may not be obtained with the chosen form of the viscoelasticity matrix in Eq. (22).

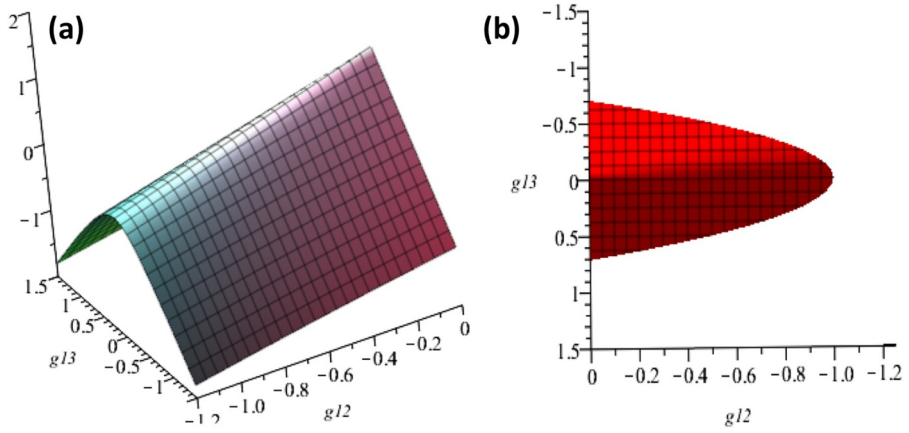


**Fig. 4.** (a) Eigenvalue $\eta_3$ as a function of $g_{12}$ and $g_{13}$. (b) The region on the plane where $\eta_3$ was positive.

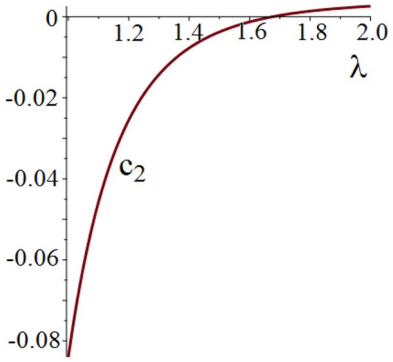


**Fig. 5.** Condition $c_2$ as a function of λ.

**Case 2**

Therefore, we consider a more complex case $g_{13} = g_{23} > 0$,

$$\mathbf{g}^v = g_{11}^{'v}\begin{bmatrix} 1 & g_{12}^v & g_{13}^v & 0 & 0 & 0 \\ g_{11}^v & g_{22}^v & g_{13}^v & 0 & 0 & 0 \\ g_{13}^v & g_{13}^v & g_{33}^v & 0 & 0 & 0 \\ 0 & 0 & 0 & g_{44}^v & 0 & 0 \\ 0 & 0 & 0 & 0 & g_{55}^v & 0 \\ 0 & 0 & 0 & 0 & 0 & g_{66}^v \end{bmatrix} \tag{26}$$

We also assume that $g_{22} = g_{33} = 1$, and the eigenvalues become as follows:

$$\eta = [1 - g_{12},\ 1 + g_{12}/2 + \sqrt{g_{12}^2 + 8g_{13}^2}/2,\ 1 + g_{12}/2 - \sqrt{g_{12}^2 + 8g_{13}^2}/2,\ g_{44},\ g_{55},\ g_{66}] \tag{27}$$

It is easy to see that only eigenvalue $\eta_3$ may become negative, and it occurs under the following condition:

$$1 + g_{12}/2 - \sqrt{g_{12}^2 + 8g_{13}^2}/2 < 0 \tag{28}$$

Fig. 4(a) shows eigenvalue $\eta_3$ as a function of coefficients $g_{12}$ and $g_{13}$. Fig. 4(b) shows the region where $\eta_3$ is positive, suggesting that any pair of $g_{12}$ and $g_{13}$ from this region correspond to a physically possible viscoelastic matrix $\mathbf{g}^v$.

Therefore, we will investigate if it is possible to satisfy simultaneously conditions $c_1$–$c_3$ which take forms as follows:

$$c_1 = 1 - g_{12}/(2\lambda^3) - g_{13}/(2\lambda^3) > 0 \tag{29}$$

$$c_2 = c_3 = 1 + g_{12} - 2g_{13}/(\lambda^6) < 0 \tag{30}$$

and $\eta_3 > = 0$. For this condition, we may consider the following minimization problem:

$$\begin{aligned} &\min c_2 = c_2(g_{12}, g_{13}) \\ &\textit{subject to } \eta_3 > 0 \end{aligned} \tag{31}$$

This problem may be solved using Maple's nonlinear optimization function NLPSolve, which yield values as follows:

$$g_{12}^{opt} = -0.996,\ \ g_{13}^{opt} = 0.0439. \tag{32}$$

With these values, the condition $c_1$ is as follows:

$$c_1(g_{12}^{opt}, g_{13}^{opt}) = \frac{1}{2}\frac{(2\lambda^3 + 0.952)}{\lambda^3}, \tag{33}$$

and it is positive for all positive λ, which corresponds to the positive viscoelastic stress contributions under uniaxial tension. Conditions $c_2 = c_3$ are as follows:

$$c_2(g_{12}^{opt}, g_{13}^{opt}) = \frac{0.004\lambda^6 - 0.088}{\lambda^6} \tag{34}$$

$c_2$ as a function of λ is shown in Fig. 5 and is negative for relatively small λ. Therefore, for all λ in the range $1 \le \lambda < 1.674$, the matrix $\mathbf{g}^v$ with coefficients in Eq. (32) will result in the negative viscoelastic contribution under a biaxial tension test. This range includes physiological values of stretch, which are estimated at about 10% in [23]. By selecting appropriate values for the coefficient $g_{11}^{'v}$ in Eq. (26) and fitting parameters in the strain energy, one may obtain viscoelastic behavior as shown in Fig. 2(b).

## 3. Discussion

We have reported a rate dependent mechanical response of tendon-to -bone insertion tissue: under the biaxial tension setting the stress decreases with the increase in strain-rate (Fig. 2), while typically under uniaxial tension setting stress increases with the increase in strain-rate. This points to an existence of a protective mechanism developed by nature to protect the insertion site and surrounding tissues from damage and rupture under high-rate loads. This mechanism is essentially anisotropic as it is activated under biaxial tension, which is closer to physiological conditions of complex multiaxial loading, and not seen under uniaxial tension tests. We therefore, hypothesized that the insertion site tissue is designed in such a way that it has optimized response to a particular, physiologic state of strain (i.e., ratio of principal stretches), and doesn't dissipate stress as good at other states of strain. However, we tested tissue only under equibiaxial test conditions, and it is not clear what exactly multiaxial state of strain the tissue is optimized for. The tissue might be optimized for the state of strain when principal stretches are not equal, and it requires further investigation. We make also a parallel with similar protective mechanisms in biological tissues' degradation under multiaxial state of strain [35–37] and with protective mechanism in vessel walls [34].

The observed mechanical viscoelastic response is unusual: viscoelasticity results in a gross negative stress contribution while typically it gives positive stress contribution, and to the best of our knowledge, it was not observed nor modeled for connective tissues. The mentioned protective effect in blood vessel wall tissue [34] was investigated in the setting when both stress and strains reduce due to the viscoelasticity, and it is not clear what will happen at the same strains, if stress will reduce at the same strain but increased strain rate and or if it will increase, as typically observed in experiments.

To put theoretical grounds under the observed phenomena we have proposed a simplest anisotropic finite strain viscoelasticity model by extending previously developed model for small strain [3]. Its simplicity allowed us to conduct analytical study and provided deep insight into the theoretical nature of the negative viscoelastic stress contribution. We found a region of parameters for this model which both satisfy thermodynamics requirements (which gives the model a physical sense) and provide negative viscoelastic contribution into stress according to the experimental observations for finite strains in the physiological limits (Figs. 4 and 5), we also found optimal values of the parameters, which maximize negative viscoelastic contribution under a given state of strain. It is important to note that for other states of strain the region of admissible values and optimal values of parameters would be different [3].

The proposed model is phenomenological and describes macroscopic viscoelastic behavior of the tendon-to-bone insertion tissues. Various microscopic mechanisms may contribute to the gross viscoelastic behavior, including the collagen fibrils viscoelasticity, dynamic cross-links between fibers, flow fluid and others. However, currently there is no data on how the hierarchical structure of the constituents and different microscopic viscoelastic mechanisms interplay to result in a gross protective viscoelastic behavior.

The proposed model is strain state dependent only in the sense of anisotropy, but is not sensitive to the magnitude of the strain, while biological tissues are typically reported to have strain-dependent behaviors, i.e., nonlinear viscoelasticity [22,29]. Our model can be generalized to account for the strain magnitude dependence, however, at this point due to very limited experimental data it wouldn't be possible to validate such a model and it is necessary to obtain more experimental data first.

Our model may be used to setup a finite element simulation of a graded material distribution to consider the effect of materials properties and structure grading on the stress level under different strain rates, as it is done for the rate independent case in Kuznetsov et al. [3]. However, this requires implementation of anisotropic viscoelasticity. Such models will be very useful to characterize and design anisotropic viscoelastic tissues and interfaces connecting dissimilar materials.

## 4. Conclusions

Tendon-to-bone insertion is highly inhomogeneous material developed by nature to dissipate stress away from the interface. Its anisotropic biomechanical functions depend intimately on the regional biochemical composition and microstructure. Importantly, this tissue has to work at different strain rates with increased efficiency at physiological strain rates and multiaxial loading. Experimental observation of reduction of stress level with increased strain rate under biaxial tension setting was reported which points on a protective viscoelastic mechanism reducing stress at higher strains. To the best of our knowledge such behavior was not reported for connective biological tissues. A theoretical anisotropic viscoelastic model for finite strains was developed and was shown to yield observed viscoelastic behavior for a set of parameters from a finite region. From this region, one may find parameters which would maximize the protective effect of stress reduction. This model may be used in finite element simulations of graded material and structural parameters in tendon-to-bone insertion and other interfaces; it will be useful to design implants for the damaged tendon-to-bone insertion and develop interfaces for dissimilar materials, taking into account rate effect and multiaxial loadings.

## Conflict of interest statement

The authors declare that they have no conflict of interest.

## Acknowledgments

The authors gratefully acknowledge Ms. Sandhya Chandrasekaran and Ms. Ashley Saltzman for their assistance for performing biaxial mechanical testing of tendon-bone insertion tissues. The authors also acknowledge Ms. Kaitlyn Barbour for her assistance for imaging histological samples. This work was supported by NSF CMMI-1400018. K. Peters was supported by the National Science Foundation while working at the foundation. Any opinion, finding, and conclusions or recommendations expressed in this material are those of the authors and do not necessarily reflect the views of the National Science Foundation.

## References

[1] G.M. Genin, A. Kent, V. Birman, B. Wopenka, J.D. Pasteris, P.J. Marquez, S. Thomopoulos, Functional grading of mineral and collagen in the attachment of tendon to bone, Biophys. J. 97 (2009) 976–985.
[2] Y. Liu, V. Birman, C. Chen, S. Thomopoulos, G.M. Genin, Mechanisms of bimaterial attachment at the interface of tendon to bone, J. Eng. Mater. Technol.-Trans. ASME (2011) 133.
[3] S. Kuznetsov, M. Pankow, K. Peters, H.-Y.S. Huang, A structural-based computational model of tendon-bone insertion tissues, Int. J. Numer. Methods Biomed. Eng. (2019).
[4] M. Benjamin, T. Kumai, S. Milz, B.M. Boszczyk, A.A. Boszczyk, J.R. Ralphs, The skeletal attachment of tendons - tendon 'entheses', Comp. Biochem. Physiol. A-Mol. Integr. Physiol. 133 (2002) 931–945.
[5] S. Thomopoulos, G.R. Williams, J.A. Gimbel, M. Favata, L.J. Soslowsky, Variation of biomechanical, structural, and compositional properties along the tendon to bone insertion site, J. Orthop. Res. 21 (2003) 413–419.
[6] Y.X. Liu, S. Thomopoulos, C.Q. Chen, V. Birman, M.J. Buehler, G.M. Genin, Modelling the mechanics of partially mineralized collagen fibrils, fibres and tissue, J. R. Soc. Interface (2014) 11.
[7] S. Chandrasekaran, M. Pankow, K. Peters, H.S. Huang, Composition and structure of porcine digital flexor tendon-bone insertion tissues, J. Biomed. Mater. Res. A 105 (2017) 3050–3058.
[8] S. Thomopoulos, J.P. Marquez, B. Weinberger, V. Birman, G.M. Genin, Collagen fiber orientation at the tendon to bone insertion and its influence on stress concentrations, J. Biomech. 39 (2006) 1842–1851.
[9] H. Bellifa, A. Bakora, A. Tounsi, A.A. Bousahla, S.R. Mahmoud, An efficient and simple four variable refined plate theory for buckling analysis of functionally graded plates, Steel Compos. Struct. 25 (2017) 257–270.
[10] H. Bellifa, K.H. Benrahou, L. Hadji, M.S.A. Houari, A. Tounsi, Bending and free vibration analysis of functionally graded plates using a simple shear deformation theory and the concept the neutral surface position, J. Braz. Soc. Mech. Sci. Eng. 38 (2016) 265–275.
[11] B. Bouderba, M.S.A. Houari, A. Tounsi, Thermomechanical bending response of FGM thick plates resting on Winkler-Pasternak elastic foundations, Steel Compos. Struct. 14 (2013) 85–104.
[12] B. Bouderba, M.S.A. Houari, A. Tounsi, S.R. Mahmoud, Thermal stability of functionally graded sandwich plates using a simple shear deformation theory, Struct. Eng. Mech. 58 (2016) 397–422.
[13] A.A. Bousahla, S. Benyoucef, A. Tounsi, S.R. Mahmoud, On thermal stability of plates with functionally graded coefficient of thermal expansion, Struct. Eng. Mech. 60 (2016) 313–335.
[14] A.A. Bousahla, M.S.A. Houari, A. Tounsi, E.A. Bedia, A novel higher order shear and normal deformation theory based on neutral surface position for bending analysis of advanced composite plates, Int. J. Comput. Methods (2014) 11.
[15] F. El-Haina, A. Bakora, A.A. Bousahla, A. Tounsi, S.R. Mahmoud, A simple analytical approach for thermal buckling of thick functionally graded sandwich plates, Struct. Eng. Mech. 63 (2017) 585–595.
[16] A. Menasria, A. Bouhadra, A. Tounsi, A.A. Bousahla, S.R. Mahmoud, A new and simple HSDT for thermal stability analysis of FG sandwich plates, Steel Compos. Struct. 25 (2017) 157–175.
[17] Y. Lanir, Constitutive equations for fibrous connective tissues, J. Biomech. 16 (1983) 1–12.
[18] Y.C. Fung, Biomechanics: Mechancial Properties of Living Tissues, Springer Verlag, New York, 1993.
[19] R. Lakes, Viscoelastic Materials, Cambridge University Press, New York, 2009.
[20] S. Reese, S. Govindjee, A theory of finite viscoelasticity and numerical aspects, Int. J. Solids Struct. 35 (1998) 3455–3482.
[21] D.P. Pioletti, L.R. Rakotomanana, Non-linear viscoelastic laws for soft biological

tissues, Eur. J. Mech. A-Solids 19 (2000) 749–759.
[22] S.E. Duenwald, R. Vanderby, R.S. Lakes, Constitutive equations for ligament and other soft tissue: evaluation by experiment, Acta Mech. 205 (2009) 23–33.
[23] S.E. Duenwald, R. Vanderby, R.S. Lakes, Viscoelastic relaxation and recovery of tendon, Ann. Biomed. Eng. 37 (2009) 1131–1140.
[24] B.B. Wheatley, D.A. Morraw, G.M. Odegard, K.R. Kaufman, T.L.H. Donahue, Skeletal muscle tensile strain dependence: hyperviscoelastic nonlinearity, J. Mech. Behav. Biomed. Mater. 53 (2016) 445–454.
[25] K. Manda, R.J. Wallace, S.Q. Xie, F. Levrero-Florencio, P. Pankaj, Nonlinear viscoelastic characterization of bovine trabecular bone, Biomech. Model. Mechanobiol. 16 (2017) 173–189.
[26] T. Iyo, Y. Maki, N. Sasaki, M. Nakata, Anisotropic viscoelastic properties of cortical bone, J. Biomech. 37 (2004) 1433–1437.
[27] T.D. Nguyen, R.E. Jones, B.L. Boyce, A nonlinear anisotropic viscoelastic model for the tensile behavior of the corneal stroma, J. Biomech. Eng.-Trans. ASME (2008) 130.
[28] Y. Zou, Y.H. Zhang, The orthotropic viscoelastic behavior of aortic elastin, Biomech. Model. Mechanobiol. 10 (2011) 613–625.
[29] M. Latorre, F.J. Montans, Strain-level dependent nonequilibrium anisotropic viscoelasticity: application to the abdominal muscle, J. Biomech. Eng.-Trans. ASME (2017) 139.
[30] J.A. Weiss, J.C. Gardiner, C. Bonifasi-Lista, Ligament material behavior is nonlinear, viscoelastic and rate-independent under shear loading, J. Biomech. 35 (2002) 943–950.
[31] B.B. Danley, H.-Y.S. Huang, Biomechanical and biochemical study of muscle-tendon-bone in porcine digital flexor tendon, ASME International Mechanical Engineering Congress and Exposition Proceeding, Houston, TX, 2015.
[32] T.C. Gasser, R.W. Ogden, G.A. Holzapfel, Hyperelastic modelling of arterial layers with distributed collagen fibre orientations, J. R. Soc. Interface 3 (2006) 15–35.
[33] R.L. Armentano, J.G. Barra, F.M. Pessana, D.O. Craiem, S. Graf, D.B. Santana, R.A. Sanchez, Smart smooth muscle spring-dampers. Smooth muscle smart filtering helps to more efficiently protect the arterial wall, IEEE Eng. Med. Biol. Mag. 26 (2007) 62–70.
[34] W. Zhang, Y. Liu, G.S. Kassab, Viscoelasticity reduces the dynamic stresses and strains in the vessel wall: implications for vessel fatigue, Am. J. Physiol. Heart Circ. Physiol. 293 (2007) H2355–H2360.
[35] J.W. Ruberti, N.J. Hallab, Strain-controlled enzymatic cleavage of collagen in loaded matrix, Biochem. Biophys. Res. Commun. 336 (2005) 483–489.
[36] M.C. Robitaille, R. Zareian, C.A. DiMarzio, K.T. Wan, J.W. Ruberti, Small-angle light scattering to detect strain-directed collagen degradation in native tissue, Interface Focus 1 (2011) 767–776.
[37] S. Huang, H.-Y.S. Huang, Biaxial stress relaxation of semilunar heart valve leaflets during simulated collagen catabolism: effects of collagenase concentration and equibiaxial strain-state, Proc. Inst. Mech. Eng. Part H J. Eng. Med. 229 (2015) 721–731.
[38] S. Huang, H.-Y.S. Huang, Prediction of matrix-to-cell stress transfer in heart valve tissues, J. Biol. Phys. (2015) 41.
[39] Z.L. Shen, H. Kahn, R. Ballarini, S.J. Eppell, Viscoelastic properties of isolated collagen fibrils, Biophys. J. 100 (2011) 3008–3015.
[40] H.T. Banks, S. Hu, Z. Kenz, A brief review of elasticity and viscoelasticity for solids, Adv. Appl. Math. Mech. 3 (2015) 1–51.
[41] K. Volokh, Mechanics of Soft Materials, Springer, 2016.
[42] O. Gultekin, G. Sommer, G.A. Holzapfel, An orthotropic viscoelastic model for the passive myocardium: continuum basis and numerical treatment, Comput. Methods Biomech. Biomed. Eng. 19 (2016) 1647–1664.
[43] J.C. Halpin, N.J. Pagano, Observations on linear anisotropic viscoelasticity, J. Compos. Mater. 2 (1968) 68–80.
[44] S.R. De Groot, P. Mazur, Non-Equilibrium Thermodynamics, Dover, Amsterdam, 1962.